

OPTICAL RADAR STUDIES OF THE ATMOSPHERE

By J. D. Lawrence, Jr., M. P. McCormick, S. H. Melfi

NASA Langley Research Center
Langley Station, Hampton, Va.

and D. P. Woodman

College of William and Mary
Williamsburg, Va.

Presented at the Fifth Symposium on Remote Sensing of Environment

FACILITY FORM 602	N 68-23359		(THRU)
	(ACCESSION NUMBER)		
	8		
	(PAGES)		
TMX-61083		(CODE)	
(NASA CR OR TMX OR AD NUMBER)		/6	
		(CATEGORY)	

Ann Arbor, Michigan
April 16-19, 1968

GPO PRICE \$ _____

CFSTI PRICE(S) \$ _____

Hard copy (HC) _____

Microfiche (MF) _____

N 10 K
TMX

OPTICAL RADAR STUDIES OF THE ATMOSPHERE

J. D. Lawrence, Jr., M. P. McCormick, S. H. Melfi

NASA Langley Research Center
Langley Station, Hampton, Virginia

and D. P. Woodman

College of William and Mary
Williamsburg, Virginia

ABSTRACT

Rigorous Mie theory calculations of clear atmosphere volume backscattering cross sections are presented for four laser wavelengths. Ruby laser radar measurements of the atmosphere are compared to a scattering model. In addition, laser radar observations of meteorological phenomena are described.

1. INTRODUCTION

A number of light scattering methods have been used to investigate the molecular and particulate content of the atmosphere. They include the searchlight probe studies of Elterman (1954) and Friedland, Katzenstein, and Zatzick (1956), the twilight scattering studies of Volz and Goody (1962) and the aerosol photometry of Newkirk and Eddy (1964). With the advent of the high powered ruby laser, optical radar studies of the atmosphere have been made by Fiocco and Smullin (1963), Fiocco and Grams (1964), Clemensha, et al. (1966), Bain and Sandford (1966), and Collis and Ligda (1964).

The purpose of this paper is to describe the optical radar investigations of the lower atmosphere currently in progress at the Langley Research Center of NASA.

2. SCATTERING OF LASER RADIATION IN THE ATMOSPHERE

The radiation backscattered by a volume element of the atmosphere located a distance S from the laser, expressed as the power incident on a coaxial receiver, is given by

$$P(S) = \frac{cEA_R q^2(S) \sigma(S)}{2S^2} \quad (1)$$

where E is the transmitted energy, A_R is the area of the receiver, $q(S)$ is the transmissivity of the atmosphere, $\sigma(S)$ is the backscattering volume cross section of a volume element located at S , and c is the velocity of light. In equation (1) the scattering volume is assumed to be a point source which requires the beam divergence and pulse width of the laser to be small.

The volume cross section and transmissivity will be interpreted according to a scattering model which assumes the atmosphere to be a mixture of molecules, described by Rayleigh theory, and aerosols, described by rigorous Mie (1908) theory.

If atmospheric absorption is neglected the transmissivity is given by

$$q(S) = \exp \left[- \int_0^{S'} \beta(s) ds \right] \quad (2)$$

where $\beta(s)$ is the sum of the molecular and aerosol scattering coefficients.

2.1 RAYLEIGH SCATTERING

The absolute Rayleigh volume cross section for backscatter from the molecular component is

$$\sigma_M = k \bar{\alpha}^2 N(z) f \quad (3)$$

where

k wave number of incident radiation, $2\pi/\lambda$

$\bar{\alpha}$ polarizability

$N(z)$ number density

and

$$f = \frac{3(2 + \Delta)}{6 - 7\Delta}$$

where Δ is the depolarization factor. For atmospheric air, G. de Vaucouleurs (1951) has measured $\Delta = 0.031$, and therefore $f = 1.054$.

The scattering coefficient for the molecular component is

$$\beta_M(z) = \int_0^{2\pi} \int_0^\pi \frac{1}{2}(1 + \cos^2\theta) \sigma_M(z) \sin\theta d\theta d\phi \quad (4)$$

2.2 LARGE PARTICLE SCATTERING

The treatment of aerosol scattering given here is similar to a more general treatment given by Bullrich (1964). Assuming that the particulate matter present in the atmosphere may be considered a polydisperse collection of homogeneous spheres of average index η , the volume cross section is given by

$$\sigma_A(z) = \int_{r_1}^{r_2} \frac{i_1(\alpha, \eta, \theta) + i_2(\alpha, \eta, \theta)}{2k^2} dn(r, z) \quad (5)$$

where $i_{1,2}(\alpha, \eta, \theta)$ are the Mie intensity functions for light with electric vector perpendicular and parallel, respectively, to the plane through the direction of propagation of the incident and scattered radiation, r is the radius of the scatterer, $\alpha = 2\pi r/\lambda$ is the particle size parameter, $dn(r, z)$ is the number density of particles with radius between r and $r + dr$ at altitude Z , and θ is the scattering angle measured between the direction of the incident and scattered radiation.

For atmospheric aerosol distributions which obey the Junge size distribution law, it may be shown that for $r_1 \ll r_2$, equation (5) may be written

$$\sigma_A(z) = \frac{\nu r_1^\nu}{2} N_A(z) \left(\frac{2\pi}{\lambda}\right)^{\nu-2} \Phi(\alpha, \eta, \theta, \nu) \quad (6)$$

where

$$\Phi(\alpha, \eta, \theta, \nu) = \int_{\alpha_1}^{\alpha_2} \frac{i_1(\alpha, \eta, \theta) + i_2(\alpha, \eta, \theta)}{\alpha^{\nu+1}} d\alpha \quad (7)$$

In equation (6), ν is the size distribution parameter, $N_A(z)$ is the total aerosol number density, and $\alpha = 2\pi r/\lambda$ is the particle size parameter.

Similarly, it may be shown that the aerosol scattering coefficient is given by

$$\beta_A(z) = \nu r_1^\nu N_A(z) \pi \left(\frac{2\pi}{\lambda}\right)^{\nu-2} K(\alpha, \eta, \nu) \quad (8)$$

where

$$K(\alpha, \eta, v) = \int_{\alpha_1}^{\alpha_2} \frac{Q_S(\alpha, \eta)}{\alpha^{v-1}} d\alpha \quad (9)$$

and

$$Q_S(\alpha, \eta) = \frac{2}{\alpha^2} \sum_{m=1}^{\infty} (2m+1) \left[|a_m|^2 + |b_m|^2 \right] \quad (10)$$

where a_m and b_m are the Mie coefficients (van de Hulst, 1957).

2.3 COMPUTATIONS

A computer program has been written to evaluate the functions Φ and K for an arbitrary choice of the aerosol parameters. The recursion relationships of Deirmendjian (1962) were used for calculation of the Mie coefficients which were terminated when $|a_m(\alpha, \eta)|$ and $|b_m(\alpha, \eta)| \leq 10^{-8}$.

The integral expressions have been calculated in increments of $\Delta\alpha = 0.1$. The functions $\Phi(\alpha, \eta, \theta, v)$ and $K(\alpha, \eta, v)$ for parameters applicable to laser backscatter from atmospheric aerosols are listed in tables I and II and can be used to calculate the backscattering cross section and scattering coefficient from equations (6) and (8).

2.4 INSTRUMENTATION

Two ruby laser radar systems have been constructed and have been used to probe the lower atmosphere.

The airborne system installed in a T-33 type jet aircraft, consists of a ruby laser transmitter and a refracting telescope receiver whose axes are aligned parallel. The laser produces pulses of approximately 0.1-joule energy and of 20-nsec duration with a beam divergence of 1 mrad. The back-scattered laser energy is collected by a receiver which has a field of view of 3 mrad and an effective collecting aperture of 0.1 meter. The optical bandwidth of the receiving system is determined by a temperature-controlled interference filter with a spectral bandwidth of 11.75 Å centered at 6943 Å. The photomultiplier detector used in this system has 16 amplifying stages and a photocathode with an S-20 spectral response. The laser output monitor is calibrated by comparison with a thermopile calorimeter and the spectral response of the receiver was determined using a standard lamp; in consequence, the airborne system can make absolute measurements of the backscattering cross section.

The ground-based system consists of a ruby laser and a 1.52-meter parabolic search light mirror positioned in a steerable mount with their axes parallel. The laser produces a 1- to 2-joule pulse of 20-nsec duration at 6943 Å, and is temperature controlled to prevent detuning into an atmospheric absorption band. A 14-stage photomultiplier detector with S-20 response is positioned near the focal plane. The optical bandwidth of the system is limited to about 700 Å by the combination of a red filter and the S-20 photocathode response. The acceptance angle of the mirror is reduced to approximately 10 mrad by a stop at the focal plane.

3. RESULTS

3.1 OBSERVATIONS OF THE CLEAR ATMOSPHERE

Typical observations of the clear atmosphere are shown in figure 1. A composite profile extending to about 22 km has been constructed from three laser shots. The solid curve in the figure is the total return calculated for the U.S. Standard 1962 Atmosphere and an aerosol component based on Rosen's (1966) direct sampling measurements above 5 km. Rosen's total number density measurements have been corrected for a lower limit 0.1 μ assuming a $v = 3$ distribution. For the altitude region below 5 km, we have assumed on the basis of Penndorf's (1954) analysis that the aerosol number decreases exponentially from the sea-level value to Rosen's value at 5 km. The experimentally determined backscattering profile has been normalized to the calculated value at 7 km.

A fast decrease in aerosol number density in the first 2 kilometers is evident; in this region the scattering is predominantly of aerosol origin. The scattering from about 2.5 to 12 kilometers appears to be predominantly of molecular origin; small increases in the absolute cross section, however, are noted throughout and indicate the presence of local concentrations of aerosols. A deviation from molecular scattering appears at about 12 kilometers and increases to about a factor of two at 19 kilometers.

Shown in figure 2 are the results of a series of simultaneous measurements of the backscattering volume cross section of a clear atmosphere by the airborne and ground systems. The profile measured with the ground-based system has been normalized to the airborne data at 7.2 km. As is evident in the figure the two sets of experimental data agree very well and in addition agree with the model calculation above 2.5 km. Below 2.5 km the measured profile deviates significantly from the calculated profile. This deviation is indicative of the aerosol concentration in the vicinity of a subsidence inversion which existed in the vicinity of 1.8 km.

3.2 OBSERVATIONS OF AEROSOL TRAPPING IN THE VICINITY OF TEMPERATURE INVERSIONS

In a region containing a temperature inversion, cool air is capped by warm air thereby trapping aerosols in the stable region at the base of the inversion. Figure 3 shows data obtained on February 28 and March 1, 1967, and the temperature profile as measured over Wallops Island. An enhancement can be seen in figure 3(a) at 15.9 km which corresponds to the height of a 4°C temperature inversion. On March 1 (fig. 3(b)) an 8°C inversion at 18 km corresponds to the enhancement at 18 km in the scattering profile.

Since the laser backscatter technique can detect very small aerosol concentrations, it constitutes an excellent method for observing the concentration in the vicinity of temperature inversions and perhaps a technique for detecting temperature inversions in both the troposphere and stratosphere.

3.3 OBSERVATION OF CLOUDS

No systematic observations of cloud systems have been made nor has any attempt been made to fit polydisperse models to our measurements. The results obtained, however, clearly demonstrate that laser radar constitutes an excellent method for observing cloud systems.

The structure evident in figure 4(a) is a high cirrus cloud extending from 9 to 12 km; also evident is an altostratus cloud at 5.85 km of thickness 300 m. The return in figure 4(b) shows a cirrus cloud system centered at approximately 11.85 km. Figure 4(c) shows another cirrus cloud which at the time of observation was stratified into three layers. The base of this system was 11.7 km, while the top was 13.35 km. Figure 4(d) is an example of the return from a dense cirrus cloud similar to that found in figure 4(a) extending from 8.7 km to 11.25 km. In addition, it should be noted that laser radar can detect clouds in their earliest stages of formation.

3.4 OBSERVATIONS OF TURBULENT REGIONS OF THE ATMOSPHERE

In a series of experiments conducted over Williamsburg, Virginia, a T-33 type jet aircraft instrumented with a recording accelerometer was directed into regions of the clear atmosphere where enhanced backscatter of ruby laser radiation was observed by an experimental ground-based pulsed ruby laser radar system. In 27 cases, established over 5 nights of observation, the aircraft encountered light turbulence (vertical acceleration generally in the range 0.10 to 0.25g) in clear air in regions of enhanced backscatter. In addition, the aircraft conducted a general search for turbulence to heights of 12 km above the field station and did not encounter turbulence in regions where no enhancement in backscattered signal was evident.

Figure 5 shows oscilloscope recordings of two such examples in which the aircraft encountered turbulence. A scattering enhancement is clearly evident in figure 5(a) from 3.3 to 4.05 km; the pilot reported light turbulence (0.1 to 0.2g) in clear air from 3.7 to 4.05 km. In figure 5(b), an enhancement extending from 2.4 to 3.1 km is evident; the pilot reported light turbulence (0.1 to 0.2g) in clear air in three layered regions extending from 2.5 to 2.8 km. Radiosonde measurements made at Wallops Island, Virginia (75 miles northeast of Williamsburg), on this evening indicated that a subsidence inversion existed at an altitude of 3.1 km; light turbulence was presented beneath this inversion.

4. REFERENCES

1. Bain, W. C.; and Sandford, M. C. W.: Light Scatter From a Laser Beam at Heights above 40 km. *J.A.T.P.* 28, 543 (1966).
2. Bullrich, K.: Scattered Radiation in the Atmosphere and the Natural Aerosol. *Advances in Geophysics* No. 10, Academic Press, New York, 99 (1964).
3. Clemsha, B. R.; Kent, G. S.; and Wright, R. H. M.: Laser Probing of the Lower Atmosphere. *Nature* 209, 184 (1966).
4. Collis, R. T. H.; and Ligda, M. G. H.: Laser Radar Echoes From the Stratified Clear Atmosphere. *Nature* 203, 508 (1964).
5. Elterman, L.: Seasonal Trends of Temperature, Density, and Pressure in the Stratosphere Obtained With the Searchlight Technique. *Geophys. Res. Papers* No. 29 (1954).

6. Fiocco, G.; and Smullin, L. D.: Detection of Scattering Layers in the Upper Atmosphere (60-140 km) by Optical Radar. *Nature* 199, 1275 (1963).
7. Fiocco, G.; and Grams, G.: Observations of the Aerosol Layer at 20 km by Optical Radar. *J.A.S.* 21, 323 (1964).
8. Friedland, S.; Katzenstein, J.; and Zatzick, M.: Pulsed Searchlighting the Atmosphere. *J. Geophys. Res.* 61, 415 (1956).
9. Newkirk, G., Jr.; and Eddy, John A.: Light Scattering by Particles in the Upper Atmosphere. *J. of the Atmos. Sci.* 21, 35 (1964).
10. Penndorf, R.: The Vertical Distribution of Mie Particles in the Troposphere. *Geophys. Res. Paper No. 25*, A.F.C.R.L., Bedford, Mass., March (1954).
11. Rosen, J. M.: Correlation of Dust and Ozone in the Stratosphere. *Nature* 209, 1343 (1966).
12. de Vaucouleurs, G.: *Ann. Phys.* 6, 211 (1951).
13. Volz, F. E.; and Goody, R. M.: The Intensity of the Twilight and Upper Atmospheric Dust. *J. of the Atmos. Sci.* 19, 385 (1962).

TABLE I. ϕ COMPUTED FOR $\theta = 180^\circ$, $n = 1.5$, $r_1 = 0.04\mu$, AND $r_2 = 10\mu$

v λ	0.3472μ	0.5300μ	0.6943μ	1.06μ
2.5	1.2050	1.1777	1.1563	1.1179
3.0	.4397	.4484	.4485	.4449
3.5	.2102	.2254	.2291	.2309
4.0	.1281	.1487	.1553	.1601

TABLE II. K COMPUTED FOR $n = 1.5$, $r_1 = 0.04\mu$, AND $r_2 = 10\mu$

v λ	0.3472	0.5300	0.6943	1.06
2.5	3.9518	3.8925	3.8389	3.7350
3.0	1.8361	1.8471	1.8450	1.8350
3.5	1.0355	1.0578	1.0629	1.0656
4.0	.6610	.6919	.7012	.7087

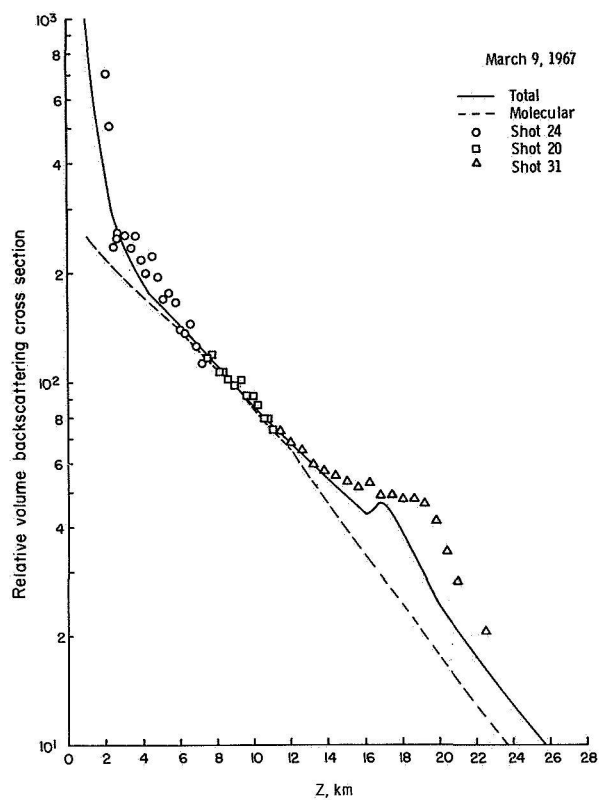


Figure 1

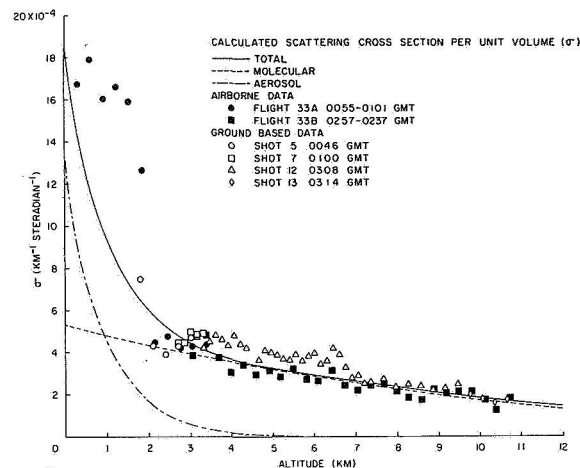


Figure 2

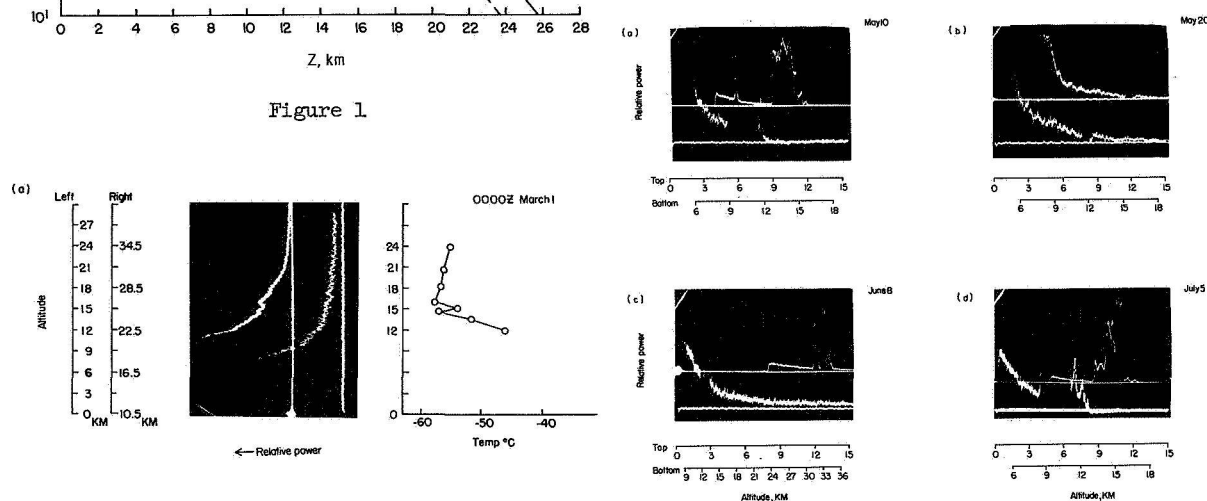


Figure 4

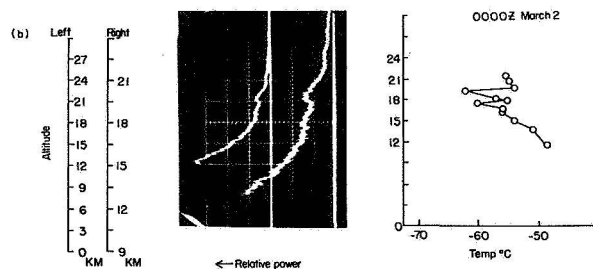


Figure 3

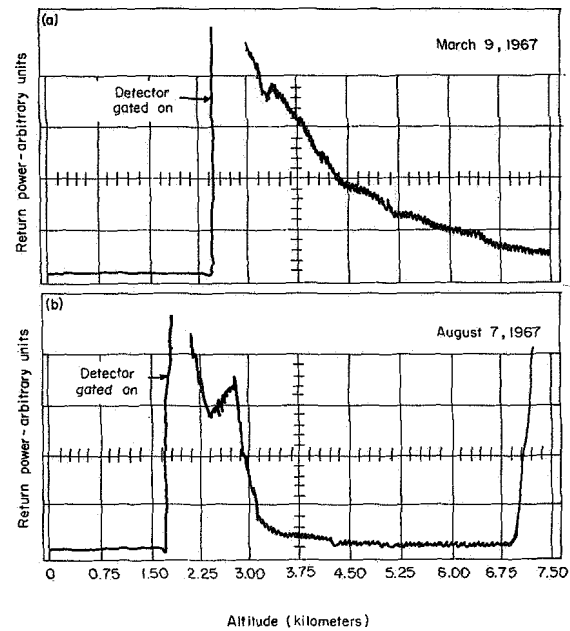


Figure 5